Journal of Biochemical and Biophysical Methods, 26 (1993) 317–334

JBBM 00999

Conformational studies on some *C1'*-branched β-D-nucleosides by ^{1}H-NMR spectroscopy and molecular mechanics calculations

J. Plavec [a], V. Fabre-Buet [b], V. Uteza [b], A. Grouiller [b] and J. Chattopadhyaya [a]

[a] *Department of Bioorganic Chemistry, Biomedical Center, University of Uppsala, Uppsala (Sweden) and* [b] *Laboratoire de Chimie Organique II, Université Lyon I, ESCIL, Villeurbanne (France)*

(Received 7 November 1992)
(Revised manuscript received 30 January 1993)
(Accepted 9 February 1993)

Summary

Solution structures of 1-(β-D-psicofuranosyl)thymine (HMT) (**5**) and 1-(1'-cyano-β-D-ribofuranosyl)-thymine (CNT) (**6**) based on $^3J_{H,H}$ coupling constants (^{1}H-NMR at 500 MHz) and nOe enhancement studies were further refined by molecular mechanics calculations using the AMBER force field. These complementary NMR-molecular mechanics studies helped us to define the torsion angles inside the NMR-defined conformational hyperspace. Atom-centered monopole charges were derived for molecular mechanics calculations by fitting the molecular electrostatic potential on freely optimized geometries of **5** and **6** using HF/3–21G level of theory by GAUSSIAN 92 program. The conformation of **5** and **6** can be summarized as follows: (i) the pseudorotational analyses showed that the North conformer is predominant in both **5** (> 70%) and **6** (97%). While the molecular mechanics could correctly predict the energetic preference of North over South type puckered sugar moiety for **5** and **6** it could not provide any clue to the fact that the 1'-CN group in CNT (**6**) drives the pseudorotational equilibrium more effectively towards North than 1'-CH_2OH in HMT (**5**). (ii) The NMR-observed preference of *anti* over *syn* conformation across the glycosyl bond in **5** and **6** was correctly shown by the energetic preference of *anti* conformers by approx. 10 kJ/mol. (iii) The populations of the staggered rotamers across C4'-C5' (γ^+, γ^t and γ^-) calculated from $^3J_{4'5'}$ and $^3J_{4'5''}$ coupling constants from NMR spectroscopy show that γ^+ and γ^t rotamers are preferred. Molecular mechanics calculations are also in an excellent agreement here with the results of solution studies: in **5** γ^+ and γ^t rotamers are equally populated and a small energy difference in potential energy is established, while in **6** the larger energy difference in potential energy is found which reflects a higher preference for γ^+ rotamer in solution. The energetic preferences found among the lowest energy conformers of **5** (North-γ^+/γ^t-*anti*-ϵ_1^t) and **6**

Correspondence address: J. Chattopadhyaya, Department of Bioorganic Chemistry, Box 581, Biomedical Center, University of Uppsala, S-751 23 Uppsala, Sweden.

(North-γ^+/γ^t-*anti*) in molecular mechanics calculations are in an excellent agreement with the preferences of the major conformers found by NMR spectroscopy in solution.

Key words: ^{1}H-NMR spectroscopy; Molecular mechanics; Conformation, North; Conformation, South

Introduction

C-branched nucleosides are of considerable biochemical importance as antibacterial, antitumor or as an antiviral agent. For example, naturally occurring nucleoside, oxetanocin A (**1**), and several of its analogues with modified 2′-substituent or aglycone, or replacement of the oxetane ring by the isosteric cyclobutane ring have produced remarkable anti-HIV activities [1]. The 2′- and 3′-*C*-hydroxymethyl-β-D-nucleosides **2** and **3**, respectively, having branched chain sugars are ring-expanded analogues of oxetanocin A (**1**) [2]. While 3′-*C*-hydroxymethyl-β-D-nucleosides **3** have shown comparable anti-HIV activities as that of oxetanocin A (**1**), the corresponding isomeric 2′-*C*-hydroxymethyl-β-D-nucleoside **2** is devoid of any significant effect [2]. On the other hand, 1′-C-hydroxymethyl-β-D-nucleosides such as psicofuranine (Angustmycin C) **4a** and decoyinine (Angustmycin A) **4b** belong to the family of naturally occurring ketose nucleosides [3]. They have pronounced antibacterial and antitumor activity and are noncompetitive inhibitors of xanthinemonophosphate aminase [4]. These biochemical activities of *C*-branched nucleosides have prompted us to investigate the structural effect of such unique single carbon homologation, as in **2**, **3**, **4a** and **4b**, on the biologically ubiquitous tetrahydrofuran ring. We herein report our structural studies on the effect of H1′ substitution in the β-D-pentofuranosyl moiety [1] by -CH_2OH and -CN as in **5** and **6** using high-field (^{1}H at 500 MHz) NMR spectroscopy and molecular mechanics calculations using Kollman's AMBER force field [22] as implemented in the MacroModel program [12,13].

Results and Discussion

^{1}H-NMR spectroscopy

The conformational analysis of 1-(β-D-psicofuranosyl)thymine (**5**; HMT) and 1-(1′-cyano-β-D-ribofuranosyl)thymine (**6**; CNT) is based on $^3J_{2'3'}$, $^3J_{3'4'}$, $^3J_{4'5'}$ and $^3J_{4'5''}$ measured through ^{1}H-NMR spectra at 500 MHz in D_2O at 298, 313, 333 and 353K (Table 1) and nOe enhancements observed through 1-D ^{1}H nOe difference spectra[1].

The population of staggered rotamers around C4′-C5′ bond (γ) in 5 and 6. The populations of the three staggered rotamers across C4′-C5′ (γ^+, γ^t and γ^-) were calculated from $^3J_{4'5'}$ and $^3J_{4'5''}$ which represent time averaged NMR coupling

[1] Note on nomenclature: in this paper the β-D-psicofuranose moiety of studied nucleosides is numbered irrespective of the proper IUPAC name as 1′-substituted β-D-ribofuranosyl sugar.

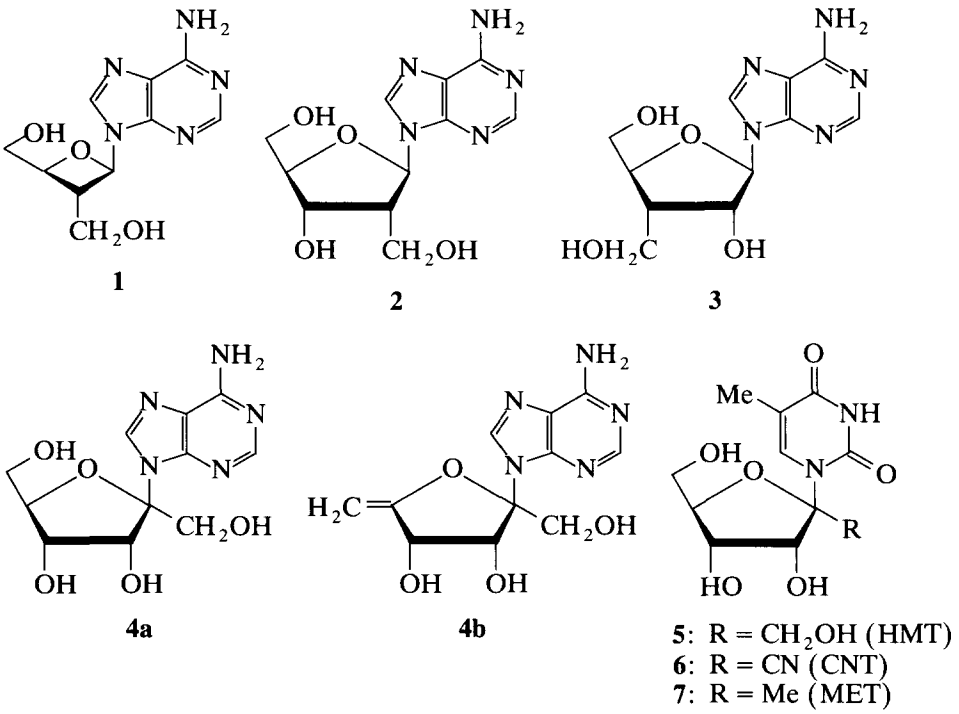

Scheme 1

constants of individual conformers and their corresponding populations [2]. Data in Table 1 show that γ^+ (47%) and γ^t (43%) rotamers are preferred in HMT (**5**) over γ^- rotamer (10%) at 298K. Upon increase of the sample temperature, the

TABLE 1

$^3J_{H,H}$ coupling constants [a] and populations of rotamers around $C_{4'}$-$C_{5'}$ bond [b] for 1-(β-D-psicofurano-syl)thymine (**5**) [c] and 1-(1'-cyano-β-D-ribofuranosyl)thymine (**6**) [d]

Compound	Temp. (K)	$J_{2'3'}$	$J_{3'4'}$	$J_{4'5'}$	$J_{4'5''}$	$\times(\gamma^+)$	$\times(\gamma^-)$	$\times(\gamma^t)$
HMT (**5**)	298	5.1	6.4	3.3	5.5	0.47	0.10	0.43
	313	5.2	6.1	3.4	5.6	0.45	0.11	0.44
	333	5.2	6.0	3.5	5.7	0.43	0.12	0.44
	353	5.3	5.7	3.6	5.8	0.41	0.14	0.45
CNT (**6**)	298	4.8	8.8	2.5	4.0	0.70	0.01	0.29
	313	4.9	8.4	2.6	4.2	0.67	0.02	0.31
	333	5.0	8.1	2.7	4.4	0.64	0.03	0.33
	353	5.1	7.7	2.8	4.5	0.62	0.04	0.33

[a] Extracted from one-dimensional ^{1}H-NMR spectra recorded at 500 MHz in D_2O[1]; [b] mole fractions were calculated using values in footnote 2; [c] δ (**5**; 298K) = 4.8 (H-2'), 4.2 (H-4'), 4.1 (H-3'), 3.8 (H-5'), 3.7 (H-5'') ppm; [d] δ (**6**; 298K) = 4.6 (H-2'), 4.35 (H-4'), 4.1 (H-3'), 4.0 (H-5'), 3.8 (H-5'') ppm.

populations of γ^t and γ^- rotamers in **5** are slightly increased, while the population of γ^+ rotamer is decreased (Table 1). For CNT (**6**), γ^+ rotamer is preferred (70%) at 298K, but an increase of the sample temperature promotes a decrease of the population of γ^+ rotamer (Table 1).

The pseudorotational analysis of the psicofuranose moiety in 5 and 6. The conformation of psicofuranose ring in HMT (**5**) and CNT (**6**) is described by using the pseudorotational concept [6–10] [3]. In this concept, the sugar ring geometry is described by two parameters: a phase angle of pseudorotation (P), which defines part of the ring which is mostly puckered and a puckering amplitude (Ψ_m), which indicates the extent of the puckering. The sugar ring, in both solution and solid states, occurs as two distinct conformations which are commonly denoted as North (C3′-*endo*, C2′-*exo*) and South (C2′-*endo*, C3′-*exo*) [6,8]. The preferred range of pseudorotational phase angle [11] for the North conformer is $0° \leqq P \leqq 36°$, while South type conformers are most commonly found in the range $144° \leqq P \leqq 190°$. The dynamic behaviour of the sugar moiety in nucleosides and nucleotides in solution is often interpreted in terms of fast conformational $N \rightleftarrows S$ equilibrium. Analysis of three-bond proton-proton coupling constants ($^3J_{H,H}$), which are a time averaged physical properties, can provide information about the geometry and population of both North and South-type conformers. Five parameters are needed to describe such a two-state conformational equilibrium: P and Ψ_m of both North and South conformer and mole fraction of one of them. Only two observables ($^3J_{2'3'}$ and $^3J_{3'4'}$) are available from the NMR measurements of the sugar ring of HMT (**5**) and CNT (**6**) which clearly can not define five unknowns. The common approach is to measure the coupling constants over a range of temperatures. The variation of sample temperature shifts the position of the $N \rightleftarrows S$ equilibrium, while the geometries of the participating conformers are expected to remain unchanged [18]. For compounds **5** and **6** each set of experimental coupling constants at a new sample temperature increases the number of observables (i.e., $^3J_{2'3'}$ and $^3J_{3'4'}$) by two, while only one extra unknown (the mole fraction at that temperature) is introduced.

Our first attempt to translate $^3J_{2'3'}$ and $^3J_{3'4'}$ into a rough structural model of the sugar ring in **5** and **6** was made by a graphical method. The proton-proton torsion angles are related to the pseudorotational parameters of the sugar moiety by two equations: $\Phi_{2'3'} = 0.2 + 1.09\ \Psi_m\cos(P)$ and $\Phi_{3'4'} = -124.9 + 1.095\ \Psi_m\cos(P + 144)$ [10]. By using the generalized Karplus equation, which relates proton-proton torsion angles and vicinal proton-proton coupling constants, we calculated dependence of $^3J_{2'3'}$ and $^3J_{3'4'}$ on the phase angle of pseudorotation (P) at certain fixed puckering amplitudes (Ψ_m). Three closed curves were generated as P was varied from 0° (North region) via 180° (South region) to 360° (North region)

[2] Limiting values for $J_{4'5'}$ and $J_{4'5''}$ in the staggered C4′-C5′ rotamers are as follows: γ^+: $J_{4'5'} = 2.4$ Hz, $J_{4'5''} = 1.3$ Hz. Rotamer γ^t: $J_{4'5'} = 2.6$ Hz, $J_{4'5''} = 10.5$ Hz. Rotamer γ^-: $J_{4'5'} = 10.6$ Hz, $J_{4'5''} = 3.8$ Hz. See also Ref. 5.

[3] The relationship between P, Ψ_m and the five endocyclic torsion angles is: $\Phi_j = \Psi_m \cdot \cos(P + (j-2) \cdot 144°)$ for $j = 0 \ldots 4$. See Ref. 6.

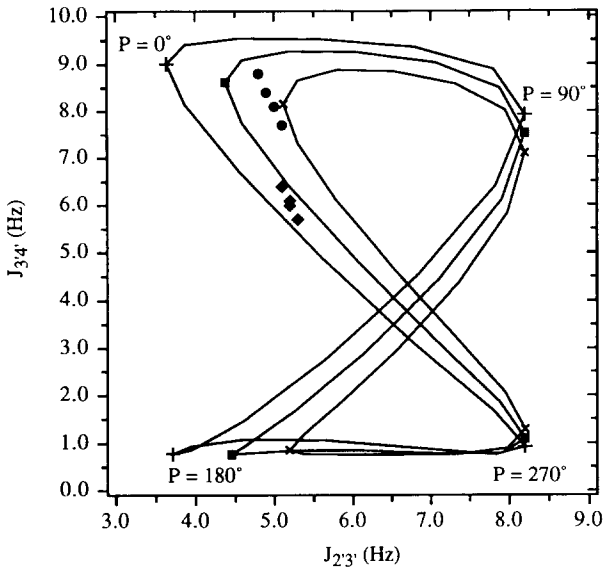

Fig. 1. Values for $^3J_{H,H}$ were calculated by varying the phase angle of pseudorotation (P) from 0–360° using Karplus-type equation as developed by Altona et al. [10] for β-D-ribo- and 2′-deoxy-β-D-ribofuranosyl nucleosides at fixed puckering amplitudes of 35° (×), 40° (■) and 45° (+). The experimental coupling constants were obtained through 500 MHz ^{1}H-NMR spectra in D_2O at four different temperatures: 1-(β-D-psicofuranosyl)thymine (**5**; ♦) and 1-(1′-cyano-β-D-ribofuranosyl)thymine (**6**; ●).

at fixed values of Ψ_m of 35°, 40° and 45° (Fig. 1). It is noteworthy that the experimental $^3J_{2'3'}$ and $^3J_{3'4'}$ for HMT (**5**)[1] (represented by ♦ in Fig. 1) and for CNT (**6**) (represented by ● in Fig. 1) clearly show variation with temperature (Table 1). Their North to South alignment shows that the sugar moiety of HMT (**5**) and CNT (**6**) is involved in the common two-state $N \rightleftarrows S$ equilibrium. Assuming that the Ψ_m is close to 40° and by constructing the conode through the experimental data points (i.e., $^3J_{2'3'}$ and $^3J_{3'4'}$) four intercepts of the conode and curve are found which define four possible two-state $N \rightleftarrows S$ equilibria for HMT (**5**): $P_N \approx 0°$ or $\sim -22°$ and $P_S \approx 134°$ or $\sim 235°$. *In all of the possible equilibria the North conformer of HMT (5) is preferred (> 70% at 298K).* If Ψ_m of North and South conformers in CNT (**6**) are assumed to be 40°, it is possible to roughly define the state of the pseudorotational equilibrium by: P_N ($\approx 18°$) $\rightleftarrows P_S$ ($\approx 130°$) and P_N ($\approx 18°$) $\rightleftarrows P_S$ ($\approx 240°$). In both feasible equilibria the North conformer of CNT (**6**) is preferred by > 90% at 298K. Clearly, these figures are only a rough estimate and conclusions that are only valid on the assumption that the modified psicofuranose ring of HMT (**5**) and CNT (**6**) is involved in the two-state equilibrium.

In an alternative analysis, the computer program PSEUROT [7] has been used for the translation of experimental coupling constants into a more precisely defined conformational picture of the β-D-psicofuranose ring in HMT (**5**) and

CNT (**6**). PSEUROT calculates the best fit of the five conformational parameters (P and Ψ_m for both North and South conformer and corresponding mole fractions) to the set of experimental $^3J_{H,H}$ coupling constants. Although the number of available experimental $^3J_{H,H}$ coupling constants (2×4 observables) is equal to number of unknowns, an unambiguous description of conformational parameters could not be obtained. The initial values of P_N and P_S were based on the different $N \rightleftarrows S$ equilibria found by the graphical approach described above (see also Fig. 1). It is self-evident that the optimized parameters are underdetemined and are influenced by experimental errors in the observed coupling constants.

The Ψ_m of both North and South conformers were fixed at 39° during PSEUROT analysis [7] of HMT (**5**). The phase angle (P) of North conformer of HMT (**5**) was found to be $-3°$, while its counterparts in the South region had $P_S = 137°$ or 232°. At 298K, populations were found to be 70% North and 30% South conformer if $P_S = 137°$ or 74% North and 26% South if $P_S = 232°$.

The PSEUROT [7] conformational analysis of the sugar ring in CNT (**6**) was run under the assumption that the contribution of the South conformer to observed $^3J_{H,H}$ coupling constants is small compared to the North conformer. Consequently, P and Ψ_m of the South conformer was fixed at $P_S = 133°$ and $P_S = 238°$, $\Psi_m = 39°$. The best fit of the conformational parameters to the set of experimental $^3J_{2'3'}$ and $^3J_{3'4'}$ for CNT (**6**) was found in the range of $P_N = 12° - 16°$ ($P_{av} = 14°$) and Ψ_m(North) = 38.2° – 39.3° (average $\Psi_m = 38.8°$). At 298K, the population of the North conformer of CNT (**6**) was found to be 97%.

The conformation around glycosyl bond (χ) in HMT (5) and CNT (6). When considering the conformation across the glycosidic bond (χ (O4'-C1'-N1-C2)) we turned to 1-D ^{1}H nuclear Overhauser enhancement (nOe) spectroscopy. 1-D ^{1}H nOe difference spectroscopy is a direct approach for the analysis of the orientation of the base relative to the sugar moiety [16]. For flexible systems, the observed nOe is a time-average of contributions from different conformers. On the basis of observed nOe enhancements upon saturation of H6 it can be concluded that the thymine is in *anti* conformation with respect to the sugar residue in **5** and **6** (for HMT (**5**): H2' (7.0%), H3' (4.6%), H5' (8.1%), H5" (8.4%) and 1'-CH_aH_b protons (10.3% and 9.4%) (Fig. 2a); for CNT (**6**) at H2' (1.6%), H3' (4.9%), H5' (7.8%) and H5" (7.0%) in (Fig. 2c)).

Molecular mechanics

Clearly, the conformational analyses of the sugar moiety in HMT (**5**) and CNT (**6**) through PSEUROT analysis of the coupling constants is greatly underdetermined (vide supra). Nevertheless, NMR data clearly showed that the North-type sugar, along with the *anti* conformation across the glycosidic bond, is by far the most predominant conformer (see also Fig. 1). At this stage, we turned our attention to molecular mechanics to probe if it can correctly predict the preferences observed for **5** and **6** in solution by NMR spectroscopy. If the molecular mechanics calculations can show the energetic preference of the North-type sugar over the South-type in HMT (**5**) and CNT (**6**) along with the preferred *anti* conformation, it will indeed serve as a powerful refinement tool to precisely define

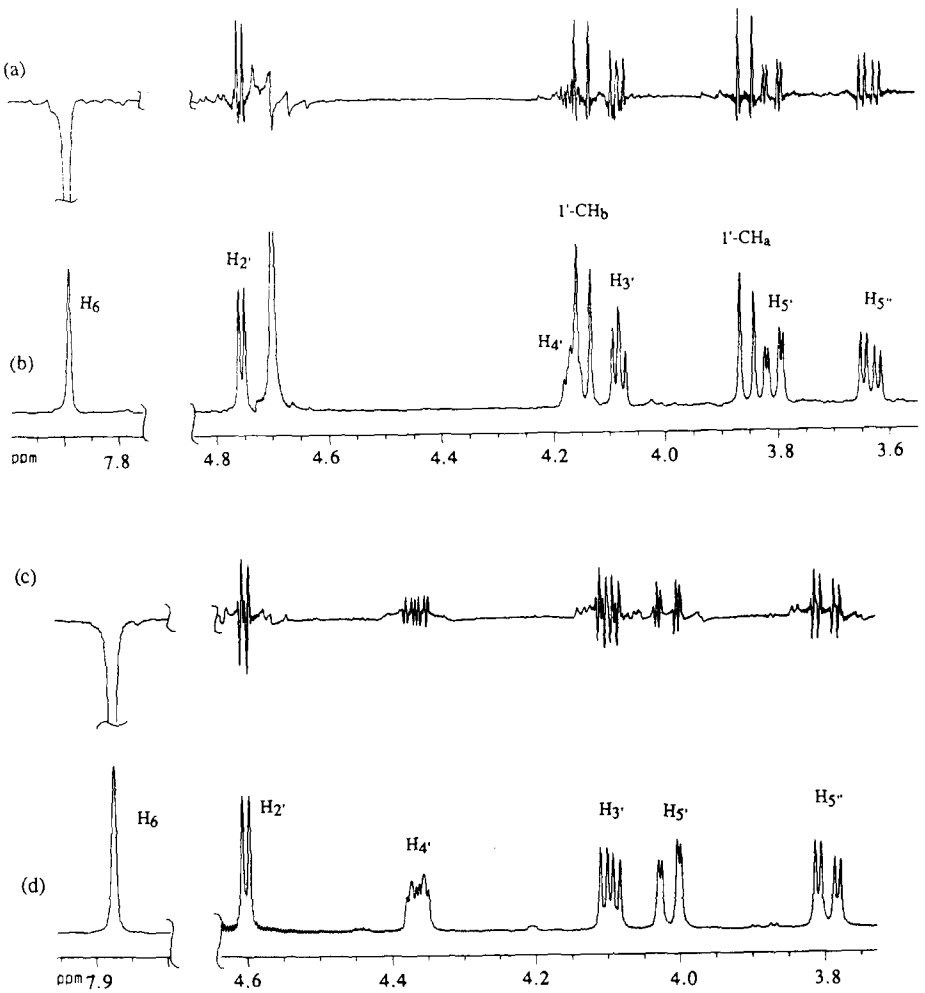

Fig. 2. 500 MHz ^{1}H-NMR spectra of 1-(β-D-psicofuranosyl)thymine (HMT, **5**) and 1-(1'-cyano-β-D-ribofuranosyl)thymine (CNT, **6**) in D_2O at 298K: (a) The nOe difference spectrum of HMT (**5**) obtained upon irradiation of H6 showing enhancements at H2′ (7.0%), 1′-CH_b (9.4%), H3′ (4.6%), 1′-CH_a (10.3%), H5′ (8.1%) and H5″ (8.4%), (b) The 1-D absorption spectrum of HMT (**5**), (c) The nOe difference spectrum of CNT (**6**) obtained upon irradiation of H6 showing enhancements at H2′ (1.6%), H3′ (4.9%), H5′ (7.8%) and H5″ (7.0%), (d) The 1-D absorption spectrum of CNT (**6**).

the torsion angles within the conformational hyperspace established though the analysis of $^3J_{H,H}$ and nOe data.

Molecular mechanics calculations for HMT (**5**) and CNT (**6**) were performed by using the MacroModel program package [12,13]. The all atom AMBER force field [22] as implemented in MacroModel V3.5a has been used [12]. A distance-dependent dielectric constant $\epsilon = 4r$ was used and 1–4 nonbonded (van der Waals and electrostatic) interactions were scaled by 2. The van der Waals and Coulumbic

TABLE 2

Ab-initio-optimized geometries of North-γ^+-*anti* conformers of 1-(β-D-psicofuranosyl)thymine (**5**) and 1-(1′-cyano-β-D-ribofuranosyl)thymine (**6**)

Entry	Compound	χ [a]	γ	P	Ψ_m	β	ϵ_3	ϵ_2	ϵ_1	ζ_1	E [b]
1	HMT (**5**)	−169.1	49.9	15.6	41.4	177.2	−152.2	−36.4	−148.5	93.4	−1052.9374953
2	CNT (**6**)	−176.7	51.3	11.7	42.1	−179.1	−153.3	−40.0	–	–	−1030.8823018

[a] χ (O4′-C1′-N1-C2), γ (O5′-C5′-C4′-C3′), P, Ψ_m, β (HO5′-O5′-C5′-C4′), ϵ_3 (C4′-C3′-O3′-HO3′), ϵ_2 (C3′-C2′-O2′-HO2′), ϵ_1 (C2′-C1′-CH_2-OH) and ζ_1 (C1′-CH_2-O-H) are expressed in degrees; [b] RHF/3-21G energy in Hartrees.

electrostatic nonbonded cutoffs were set at 25.0 Å, which exceeds the size of the molecule in **5** and **6**. In the energy minimization with truncated Newton conjugate gradient minimizer (TNCG) [15] the structure was assumed converged if the energy gradient was < 0.004 kJ/mol.Å.

The point charges used in the calculation of the electrostatic term of the total potential energy were adjusted to respond to the changes made by introducing CH_2OH and CN substituents at C1′ of ordinary β-D-ribofuranose moiety. This was done by *ab initio* quantum mechanical calculations in two steps: (i) both compounds **5** and **6** were freely energy optimized with the starting conformation of North-γ^+-*anti* at HF/3–21G level of theory by GAUSSIAN 92 program, [23] and the resulting optimized geometries are shown in Table 2.

In step (ii), the atom-centered monopole charges were derived by fitting the molecular electotrostatic potential (ESP fit method) by Singh-Merz-Kollman method [20,21] as implemented in GAUSSIAN 92 program [23]. To avoid the problem of determining a set of nonbonded parameters that could be used with the charges to give acceptable geometries and energies we attempted to produce the charges that were comparable to charges of standard nucleic acid residues on the parts of the molecule where modifications were not made [20]. For that reason the charge fit for **5** and **6** was performed using STO-3G basis set on our HF/3–21G optimized geometries (presented in Table 2) of complete molecules and the atom van der Waals radii were taken from AMBER [22]. The point charges for all the atoms in **5** and **6** are presented together with corresponding atom types in Table 3.

The puckering of the psicofuranose moiety in HMT (5) and CNT (6). The steric energy was calculated for various phase angles of pseudorotation in **5** and **6**. The full pseudorotation cycle was explored by varying the phase angle from $P = 0°$ to 340° in 20° resolution. The torsional constraints were imposed on ν_0 (C4′-O4′-C1′-C2′) and ν_2 (C1′-C2′-C3′-C4′) to give appropriate P at $\Psi_m = 39°$ (as found by PSEUROT analysis, *vide supra*). For both **5** and **6** two sets of calculations were performed in which γ (O5′-C5′-C4′-C3′) was placed to *gauche*$^+$ ($\gamma = 60°$) and *trans* ($\gamma = 180°$) region of conformational space which corresponds to the preferred staggered modes found through analysis of $^3J_{4'5'}$ and $^3J_{4'5''}$ (Table 1). The orientation around glycosyl bond in all starting conformers was *anti* ($\chi = 180°$). It is clear

TABLE 3

Atom types [a] and electrostatic potential derived partial atomic charges [b] used in molecular modeling of HMT (**5**) and CNT (**6**) by MacroModel's implementation of AMBER force field

Atom name	Atom type [a]	Charge [b] HMT (**5**)	Charge [b] CNT (**6**)	Atom name	Atom type [a]	Charge [b] HMT (**5**)	Charge [b] CNT (**6**)
N1	N2 (25)	−0.808	−0.543	C4′	C3 (3)	0.030	0.003
C2	C2 (2)	0.938	0.943	H4′	H1 (41)	0.046	0.086
O2	O2 (15)	−0.530	−0.501	O4′	O3 (16)	−0.412	−0.275
N3	N2 (25)	−0.839	−0.869	C3′	C3 (3)	0.355	0.392
H3	H3 (43)	0.337	0.347	H3′	H1 (41)	−0.035	−0.001
C4	C2 (2)	0.868	0.869	O3′	O3 (16)	−0.541	−0.535
O4	O2 (15)	−0.478	−0.470	HO3′	H2 (42)	0.320	0.318
C5	C2 (2)	−0.227	−0.237	C2′	C3 (3)	0.059	0.063
C5-$\underline{C}H_3$	C3 (3)	−0.456	−0.420	H2′	H1 (41)	0.037	0.092
Ha-CH2-C5	H1 (41)	0.135	0.128	O2′	O3 (16)	−0.560	−0.483
Hb-CH2-C5	H1 (41)	0.124	0.114	HO2′	H2 (42)	0.340	0.330
Hc-CH2-C5	H1 (41)	0.128	0.124	C1′	C3 (3)	0.763	−0.046
C6	C2 (2)	0.296	0.237	$\underline{C}H_2$-C1′	C3 (3)	0.129	–
H6	H1 (41)	0.081	0.126	O-CH_2-C1′	O3 (16)	−0.516	–
O5′	O3 (16)	−0.444	−0.450	Ha-CH-C1′	H1 (41)	0.016	–
HO5′	H2 (42)	0.294	0.302	Hb-CH-C1′	H1 (41)	0.019	–
C5′	C3 (3)	0.161	0.131	H-OCH_2-C1′	H2 (42)	0.327	–
H5′	H1 (41)	0.032	0.044	C1′-$\underline{C}N$	C1 (1)	–	0.644
H5″	H1 (41)	0.011	0.023	C1′-$\underline{C}N$	N1 (24)	–	−0.483

[a] Atom types (type numbers) refer to MacroModel [13] and represent only the chemical element and hybridization (which is not the case in 'original' AMBER [22]; [b] Net atomic point charges were obtained by ab-initio quantum mechanical calculations using a least-square fit of the electrostatic potential (ESP) to that of the charge model by Singh-Merz-Kollman method [20,21] as implemented in GAUSSIAN 92 (see text) [23].

that the orientation of the 2′-OH, 3′-OH and 5′-OH in **5** and **6** as well as 1′-CH_2*OH* in HMT (**5**) and their strong electrostatic properties can strongly effect the sugar pseudorotation profile [19]. In the absence of the water, which would compete for the intramolecular hydrogen bonding of these hydroxyl groups, we have decided to constrain the orientation of 3′-OH and 2′-OH to an orientation in which a hydrogen bond between 3′-O $\cdots$ H-*O*-2′ is formed [24,25] (by torsional constraints on ϵ_3 (C4′-C3′-O3′-*H*O3′) and ϵ_2 (C3′-C2′-O2′-*H*O2′) to values found by ab-initio calculations presented in Table 2). Such constraints are also supported by the thermometric titration curves for titration of aqueous solution of ribose and several nucleoside derivatives by alkali [24] and X-ray crystallographic studies [25]. It may be noted that the constraint energy in all energy minimized (converged) structures was < 0.2 kJ/mol which represents $< 0.5\%$ of total potential energy and this constraint energy comes mainly from constraints on endocyclic torsion angles ν_0 and ν_2. The orientation of 5′-OH was trans (β (*H*O5′-O5′-C5′-C4′) = 180°) and was free during energy minimization. In HMT (**5**), ζ_1 (C1′-*C*H_2-O-H)

was set to 180° in all of the starting conformers. All energy profiles for **5** and **6** (shown in Fig. 3a and 3b) were obtained by constraining ν_0, ν_2, ϵ_3 and ϵ_2 while the rest of the molecule was optimized freely.

For HMT (**5**), two energy minima were found for both *gauche*$^+$ and *trans* orientations around C4′-C5′ bond (Fig. 3a). The minima in the North region at $P = 0°$ are energetically prefered over minima in the South region at $P = 220°$ by 6.5 kJ/mol in γ^+ and 1.7 kJ/mol in γ^t. In γ^+ region there is second local minimum at $P = 140°$ which is 9.1 kJ/mol higher than minimum at $P = 0°$ (Fig. 3a). Two energy minima found for CNT (**6**) in the North region at $P = 20°$ are energetically preferred over minima in the South region at $P = 140°$ by 1.7 kJ/mol in γ^+ and at $P = 220°$ by 2.0 kJ/mol in γ^t mode (Fig. 3b). The pseudorotational barriers for conversion from South to North at $P = 100°$ in HMT (**5**) are 5.8 kJ/mol in γ^+ and 10.1 kJ/mol in γ^t region (Fig. 3a) and in CNT (**6**) 5.0 kJ/mol (γ^+) and 4.0 kJ/mol (γ^t) (Fig. 3b).

The PSEUROT analyses of $^3J_{H,H}$ in **5**, **6** and **7** [17] (vide supra) established > 70% preference for North type sugar geometry for HMT (**5**), 97% preference for CNT (**6**) and 80% preference for MET (**7**) [17] ($P = -3°$ and $\Psi_m = 38.5°$). In this work we have expanded molecular mechanics calculation on MET (**7**) [17] by using ESP charges which were obtained as described for **5** and **6** [4,5]. A close correspondence was found between the lowest energy conformers obtained through MacroModel's AMBER force field calculations presented in Fig. 3a and 3b and NMR-PSEUROT derived pseudorotational parameters for all three compounds **5–7** [17] [6]. The preference for North conformers in **5–7** is nicely reflected in molecular mechanics calculations. From the analyses of $^3J_{H,H}$ it is clear that the cyano group at C1′ in CNT (**6**) drives equilibria towards North more than hydroxymethyl or methyl group in HMT (**5**) and MET (**7**), respectively (Fig. 1 and Ref. 17). This observation can not be explained through our present molecular mechanics calculations on **5–7** as the energetic preference for North over South type puckered sugar moiety is the smallest in CNT (**6**).

---

[4] The geometry of the freely HF/3–21G optimized (*N*-γ^+-*anti*) conformer of MET (**7**) is: $\chi = -179.4°$, $\gamma = 51.5°$, $P = 10.8°$, $\Psi_m = 42.0°$, $\beta = -178.8°$, $\epsilon_3 = -154.6°$ and $\epsilon_2 = -38.4°$. RHF/3–21G energy is −978.5078267 Hartree.

[5] The point charges for all the atoms in MET (**7**) with corresponding MacroModel's atom types in brackets are: N1(N2 (25)) = −0.718, C2 (C2 (2)) = 0.963, O2 (O2 (15)) = −0.525, N3 (N2 (25)) = −0.871, H3 (H3 (43)) = 0.342, C4 (C2 (2)) = 0.873, O4 (O2 (15)) = −0.479, C5 (C2 (2)) = −0.241, C5-*C*H$_3$ (C3 (3)) = −0.477, *Ha*-CH2-C5 (H1 (41)) = 0.141, *Hb*-CH2-C5 (H1 (41)) = 0.132, *Hc*-CH2-C5 (H1 (41)) = 0.133, C6 (C2 (2)) = 0.282, H6 (H1 (41)) = 0.083, O5′ (O3 (16)) = −0.438, *H*O5′ (H2 (42)) = 0.294, C5′ (C3 (3)) = 0.124, H5′ (H1 (41)) = 0.036, H5″ (H1 (41)) = 0.013, C4′ (C3 (3)) = 0.079, H4′ (H1 (41)) = 0.039, O4′ (O3 (16)) = −0.400, C3′ (C3 (3)) = 0.427, H3′ (H1 (41)) = −0.060, O3′ (O3 (16)) = −0.557, *H*O3′ (H2 (42)) = 0.320, C2′(C3 (3)) = −0.009, H2′ (H1 (41)) = 0.059, O2′ (O3 (16)) = −0.494, *H*O2′ (H2 (42)) = 0.321, C1′ (C3 (3)) = 0.711, C1′-*C*H$_3$ (C3 (3)) = −0.549, *Ha*-CH2C1′ (H1 (41)) = 0.146, *Hb*-CH2C1′ (H1 (41)) = 0.142, *Hc*-CH2C1′ (H1 (41)) = 0.158.

[6] The energetic preference for North type sugar at $P = 0°$ over South type at $P = 220°$ in MET (**7**) is 5.8 kJ/mol for γ^+ and 0.9 kJ/mol for γ^t region. The pseudorotational barriers for conversion from South to North through the East in MET (**7**) are 7.1 and 11.7 kJ/mol in γ^+ and γ^t region, respectively.

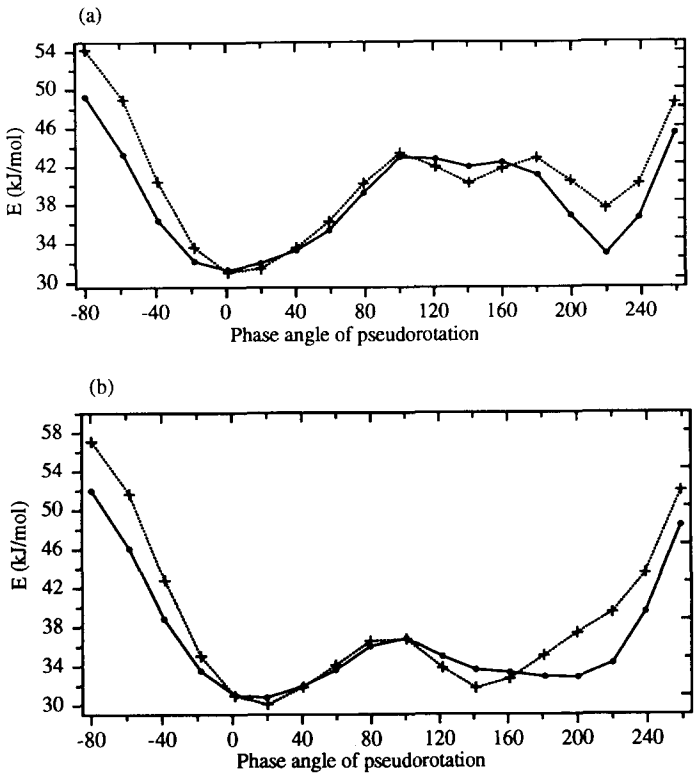

Fig. 3. The plot of the potential energy as a function of the phase angle of pseudorotation (P) for (a) 1-(β-D-psicofuranosyl)thymine (HMT, **5**) and (b) 1-(1′-cyano-β-D-ribofuranosyl)thymine (CNT, **6**). The profiles shown above were obtained through energy minimization of conformers with different P in the range $P = 0$–$340°$ in 20° resolution. Torsional constraints on ν_0 (C4′-O4′-C1′-C2′) and ν_2 (C1′-C2′-C3′-C4′) were used to give appropriate P at $\Psi_m = 39°$. The orientation around the glycosyl bond is *anti* in all of the starting conformers of **5** and **6**. 3′-OH and 2′-OH groups are restrained to orientation in which the H-bond between 3′-O and 2′-OH is formed [24,25] by constraints on ϵ_3 (C4′-C3′-O3′-*H*O3′) and ϵ_2 (C3′-C2′-O2′-*H*O2′) (see text). The orientation of 5′-OH is *trans* (β (*H*O5′-O5′-C5′-C4′) = 180°). In **5**, ζ_1 (C1′-*C*H_2-O-H) is 180° in all of the starting conformers. All energy profiles for **5** and **6** were obtained by constraining ν_0, ν_2, ϵ_3 and ϵ_2 while the rest of the molecule was optimized freely. For both **5** and **6** two graphs are shown corresponding to two distinct orientation around C4′-C5′ bond (γ (O5′-C5′-C4′-C3′) in *gauche*$^+$ (dotted line labelled with +) and *trans* (solid line labelled with •) regions): (a): For (**5**) the lowest energy minima in the North region at $P = 0°$ are found for both *gauche*$^+$ and *trans* orientations around C4′-C5′ bond. They are energetically prefered over minima in the South region at $P = 220°$ by 6.5 kJ/mol in γ^+ and 1.7 kJ/mol in γ^t region. In γ^+ region there is another local minimum at $P = 140°$ which is 9.1 kJ/mol higher than minimum at $P = 0°$. (b): Two energy minima found for (**6**) in the North region at $P = 20°$ are energetically preferred over minima in the South region at $P = 140°$ by 1.7 kJ/mol in γ^+ and at $P = 220°$ by 2.0 kJ/mol in γ^t mode. The pseudorotational barriers for conversion from South to North at $P = 100°$ in **5** are 5.8 kJ/mol in γ^+ and 10.1 kJ/mol in γ^t region and in **6** 5.0 kJ/mol (γ^+) and 4.0 kJ/mol (γ^t).

The orientation of the exocyclic groups (χ, γ, ϵ_1) in 5 and 6. For HMT (**5**), a conformational grid search was performed by simultaneously varying χ (O4′-C1′-N1-C2) and ϵ_1 (C2′-C1′-CH_2-O*H*) in γ^+ and γ^t region in both North and South type puckered sugar geometries while monitoring the change in the potential energy. At every point of potential energy surface the whole molecule was fully optimized, except the orientation of 3′-OH and 2′-OH which were placed in the orientation where 3′-O · · · H-*O*-2′ hydrogen bond is possible (vide supra, ϵ_3 and ϵ_2 were constrained in addition to the two torsions varied during bidimensional searches of conformational space). For HMT (**5**), four searches were performed in which χ and ϵ_1 were varied [14] from 0° to 340° in 20° resolution (Fig. 4a-d). The contours show a lowest energy minimum at $\chi = 180°$ and $\epsilon_1 = 180°$ in (North-γ^+) region (Fig. 4a; $E = 31.8$ kJ/mol), in (North-γ^t) region (Fig. 4b; $E = 32.1$ kJ/mol), in (South-γ^+) region (Fig. 4c; $E = 37.1$ kJ/mol) and in (South-γ^t) region (Fig. 4d; $E = 34.3$ kJ/mol). A bidimensional study where the orientation around glycosidic and C4′-C5′ bond were simultaneously considered was performed *for CNT (6) when the lowest energy minima with the North puckered sugar were found at $\chi = 180°$ and $\gamma = 60°$ ($E = 31.0$ kJ/mol) and at $\chi = 180°$ and $\gamma = 180°$ only 0.6 kJ/mol above ($E = 31.6$ kJ/mol; Fig. 5a).* For South conformers of CNT (**6**), the lowest energy minima were found at $\chi = 200°$ and $\gamma = 60°$ ($E = 31.7$ kJ/mol) and $\chi = 200°$ and $\gamma = 180°$ which has 1.0 kJ/mol higher energy ($E = 32.7$ kJ/mol; Fig. 5b).

Finally, 324 conformers of HMT (**5**) (χ and ϵ_1 in the range 0° to 340° in 20° resolution) in (North-γ^+), (North-γ^t), (South-γ^+) and (South-γ^t) region of the conformational space were energy minimized without constraints on χ and ϵ_1. The 3′-O · · · H-*O*-2′ hydrogen bond was restrained in all the minimized conformers by constraining ϵ_3 and ϵ_2. *The results presented in Table 4 show that the lowest energy minimum for HMT (5) is found for conformer in (North-γ^+-anti-ϵ_1^t) region of conformational space (entry 1, Table 4).* The preference over (North-γ^t-*anti*-ϵ_1^t) conformer is 0.3 kJ/mol (entry 2 in the middle of Table 4). Two sets of local minima were found in the *syn* regions of conformational space for HMT (**5**) some which are of comparable energy within 1 to 2 kJ/mol (Fig. 4a–d) [7].

The conformational search with different starting points in χ–γ plane for North and South puckered CNT (**6**) established the lowest energy minima for (North-γ^+-*anti*) conformer ($E = 29.9$ kJ/mol; entry 1 in Table 5). The preference over (North-γ^t-*anti*) conformer is 0.7 kJ/mol ($E = 30.6$ kJ/mol; entry 2 in Table 5).

[7] The second local minima in *syn* regions of conformational space for HMT (**6**) with higher energy than those presented in Table 4 are: (1) $\chi = -3°$, $\gamma = 57°$, $\epsilon_1 = 70°$, $P = 24°$, $\Psi_m = 42°$ (54.2 kJ/mol), (2) $\chi = -41°$, $\gamma = -179°$, $\epsilon_1 = 66°$, $P = -32°$, $\Psi_m = 45°$ (52.1 kJ/mol), (3) $\chi = 40°$, $\gamma = 58°$, $\epsilon_1 = -177°$, $P = 48°$, $\Psi_m = 41°$ (45.7 kJ/mol), (4) $\chi = 29°$, $\gamma = -178°$, $\epsilon_1 = -173°$, $P = 35°$, $\Psi_m = 41°$ (42.8 kJ/mol), (5) $\chi = 20°$, $\gamma = 56°$, $\epsilon_1 = -171°$, $P = 147°$, $\Psi_m = 35°$ (45.9 kJ/mol), (6) $\chi = 36°$, $\gamma = -178°$, $\epsilon_1 = -175°$, $P = 142°$, $\Psi_m = 35°$ (46.2 kJ/mol), (7) $\chi = 60°$, $\gamma = 60°$, $\epsilon_1 = -64°$, $P = 57°$, $\Psi_m = 39°$ (58.6 kJ/mol), (8) $\chi = 59°$, $\gamma = -177°$, $\epsilon_1 = -63°$, $P = 57°$, $\Psi_m = 39°$ (56.5 kJ/mol), (9) $\chi = -35°$, $\gamma = 62°$, $\epsilon_1 = -74°$, $P = 201°$, $\Psi_m = 34°$ (49.8 kJ/mol), (10) $\chi = 40°$, $\gamma = -179°$, $\epsilon_1 = -46°$, $P = 145°$, $\Psi_m = 38°$ (60.0 kJ/mol).

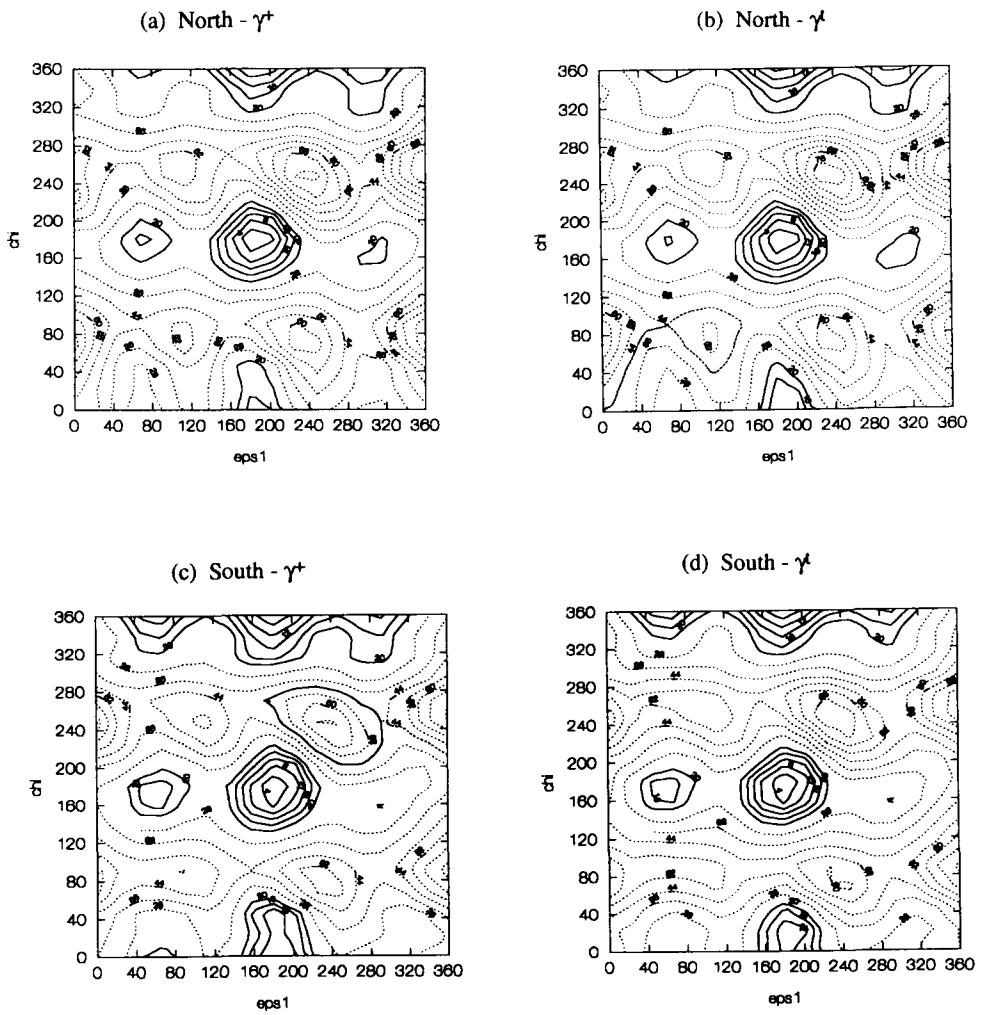

Fig. 4. Plot of energy contours in χ (O4′-C1′-N9-C2)-ϵ_1 (C2′-C1′-CH2-OH) plane for HMT (**5**). At every point of potential energy surface the whole molecule was fully optimized, except the orientation of 3′-OH and 2′-OH which were restrained to geometry where 3′-O $\cdots$ H-O2′ hydrogen bond is possible (ϵ_3 and ϵ_2 were constrained in addition to χ and ϵ_1 which were varied during grid searches of the conformational space). The contours show the lowest energy minimum at $\chi = 180°$ and $\epsilon_1 = 180°$ in the (North-γ^+) region (panel a; $E = 31.8$ kJ/mol), in the (North-γ^t) region (panel b; $E = 32.1$ kJ/mol), in the (South-γ^+) region (panel c; $E = 37.1$ kJ/mol) and in the (South-γ^t) region (panel d; $E = 34.3$ kJ/mol). In all four graphs the energy contours represented with solid line are spaced by 4.0 kJ/mol and are shown up to 20.0 kJ/mol above the lowest energy minimum in that region of conformational space. The energy contours shown by dotted line start at 28.0 kJ/mol and are incremented by 8.0 kJ/mol.

The lowest energy minima in the *syn* region of conformational place are characterized by 5 to 11 kJ/mol higher potential energy than corresponding minima in the *anti* range. Actually, two sets of local minima (only the lowest energy minima are

presented in Table 5, entries 7–12) were found in the *syn* region for CNT (**6**) which were within 1 to 2 kJ/mol (Fig. 5a, b) [8].

On the basis of our 1-D ^{1}H nOe measurements, we established that the thymine is *anti* relative to the sugar moiety in compounds **5–7**. In HMT (**5**) and MET (**7**) [17], γ^+ and γ^t rotamers are preferred over γ^- and approximately equally populated (Table 1 and Ref. 17). Molecular mechanics calculations are clearly consistent with those NMR observations (Tables 4,5 and footnotes [9,10]). The more precisely defined torsions for χ and γ by molecular mechanics calculations in the NMR-defined hyperspace show the power of combined NMR-molecular mechanics approach in the conformational analysis of **5–7**. In CNT (**6**) the population of γ^+ and γ^t rotamers at 298K are 70% and 29%, respectively (Table 1). The energetic preference for (North-γ^+-*anti*) conformer of CNT (**6**) over (North-γ^t-*anti*) is 0.7 kJ/mol (entries 1 and 2 in Table 5). Note, the smaller energy difference of 0.3 and 0.1 kJ/mol between (North-γ^+-*anti*) and (North-γ^t-*anti*) conformers in the case of HMT (**5**) and MET (**7**), respectively (Table 4 and footnote [10]) which is in good correlation with the experimental data shown in Table 1.

The protons of 1′-CH_2OH group in **5** appeared in ^{1}H-NMR spectrum as two separate doublets (Fig. 2b) with distinctly different chemical shifts suggesting a restricted rotation across C1′-CH_2 bond[1]. Two methylenic protons are therefore located in two different enviroments of diamagnetic anisotropic zone of the

[8] The higher energy local minima (compare with Table 5) for CNT (**6**) in *syn* regions are: (1) $\chi = 46°$, $\gamma = 58°$, $P = 56°$, $\Psi_m = 41°$ (42.2 kJ/mol), (2) $\chi = -57°$, $\gamma = -178°$, $P = -38°$, $\Psi_m = 43°$ (42.1 kJ/mol), (3) $\chi = -57°$, $\gamma = -62°$, $P = -39°$, $\Psi_m = 43°$ (45.3 kJ/mol), (4) $\chi = 39°$, $\gamma = -179°$, $P = 152°$, $\Psi_m = 37°$ (39.3 kJ/mol) and (5) $\chi = 39°$, $\gamma = -67°$, $P = 156°$, $\Psi_m = 37°$ (41.9 kJ/mol).

[9] A grid search on MET (**7**) where the orientation around glycosidic and C4′ − C5′ bond (324 conformers with χ and γ varied in the range 0° to 340° in 20° resolution) were simultaneously considered (χ, γ, ϵ_3 and ϵ_2 were constrained, while the rest of the molecule was optimized freely) established the lowest energy minimum for the North puckered sugar at $\chi = 180°$ and $\gamma = 60°$ ($E = 29.6$ kJ/mol). The minimum at $\chi = 180°$ and $\gamma = 180°$ has 0.2 kJ/mol higher energy ($E = 29.8$ kJ/mol). The South puckered MET (**7**) showed the lowest energy minimum at $\chi = 160°$ and $\gamma = 180°$ ($E = 32.2$ kJ/mol).

[10] The energy minimization (ϵ_3 and ϵ_2 were constrained in order to achieve 3′-O ··· H-O2′ H-bond) of 324 conformers of MET (**7**) (χ and γ varied in the range 0° to 340° with 20° resolution) with both North and South type puckered sugar geometry showed two lowest energy minima for (North-γ^+-*anti*) ($E = 29.5$ kJ/mol) and (North-γ^t-*anti*) ($E = 29.6$ kJ/mol) conformers. The energetic preference over (South-γ^t-*anti*) conformer is 0.9 and 0.8 kJ/mol, respectively. The local minima for MET (**7**) are: (1) $\chi = 178°$, $\gamma = 58°$, $P = 7°$, $\Psi_m = 41°$ (29.5 kJ/mol), (2) $\chi = 178°$, $\gamma = 182°$, $P = -1°$, $\Psi_m = 41°$ (29.6 kJ/mol), (3) $\chi = 177°$, $\gamma = -64°$, $P = -4°$, $\Psi_m = 41°$ (34.6 kJ/mol), (4) $\chi = 171°$, $\gamma = 54°$, $P = 218°$, $\Psi_m = 34°$ (34.0 kJ/mol), (5) $\chi = 170°$, $\gamma = 180°$, $P = 222°$, $\Psi_m = 40°$ (30.4 kJ/mol), (6) $\chi = 170°$, $\gamma = -67°$, $P = 222°$, $\Psi_m = 40°$ (36.2 kJ/mol), (7) $\chi = -43°$, $\gamma = 58°$, $P = -27°$, $\Psi_m = 45°$ (37.5 kJ/mol), (8) $\chi = 49°$, $\gamma = 59°$, $P = 53°$, $\Psi_m = 39°$ (38.7 kJ/mol), (9) $\chi = 46°$, $\gamma = -177°$, $P = 50°$, $\Psi_m = 39°$ (36.2 kJ/mol), (10) $\chi = -40°$, $\gamma = -179°$, $P = -34°$, $\Psi_m = 45°$ (37.7 kJ/mol), (11) $\chi = 46°$, $\gamma = -64°$, $P = 50°$, $\Psi_m = 39°$ (41.1 kJ/mol), (12) $\chi = -26°$, $\gamma = -64°$, $P = -27°$, $\Psi_m = 44°$ (41.4 kJ/mol), (13) $\chi = -17°$, $\gamma = 58°$, $P = 214°$, $\Psi_m = 34°$ (38.6 kJ/mol), (14) $\chi = 36°$, $\gamma = 55°$, $P = 138°$, $\Psi_m = 37°$ (41.5 kJ/mol), (15) $\chi = -23°$, $\gamma = -179°$, $P = 218°$, $\Psi_m = 40°$ (37.0 kJ/mol), (16) $\chi = 41°$, $\gamma = -178°$, $P = 142°$, $\Psi_m = 34°$ (40.7 kJ/mol), (17) $\chi = -19°$, $\gamma = -65°$, $P = 219°$, $\Psi_m = 40°$ (41.3 kJ/mol), (18) $\chi = 41°$, $\gamma = -66°$, $P = 144°$, $\Psi_m = 34°$ (44.2 kJ/mol).

TABLE 4

Local minima established for 1-(β-D-psicofuranosyl)thymine (HMT) (**5**)

Entry	Conformer	ϵ_1-*gauche* $^+$						ϵ_1-*trans*						ϵ_1-*gauche* $^-$					
		E [a]	χ [b]	γ	ϵ_1	P	Ψ_m	E [a]	χ	γ	ϵ_1	P	Ψ_m	E [a]	χ	γ	ϵ_1	P	Ψ_m
1	N γ^+ *anti*	39.9	−179	58	73	15	41	30.9	179	58	−171	7	41	45.4	166	58	−54	−11	43
2	N γ^t *anti*	40.7	−179	−178	73	10	41	31.2	179	−178	−171	0	41	44.8	164	180	−56	−22	44
3	S γ^+ *anti*	43.2	172	53	60	219	33	36.2	173	54	180	216	34	49.5	162	57	−73	215	35
4	S γ^t *anti*	40.0	170	179	60	223	39	32.9	171	180	180	222	40	45.6	162	179	−72	222	41
5	N γ^+ *syn*	51.6	−43	58	67	−25	45	43.1	−25	55	−175	−18	43	43.5	−46	58	−63	−27	45
6	N γ^t *syn*	51.5	32	−177	71	37	39	42.6	−22	−178	−175	−21	44	43.6	−45	−179	−63	−35	46
7	S γ^+ *syn*	49.9	−22	57	59	218	33	43.4	−17	58	179	213	34	47.9	−48	59	−78	122	40
8	S γ^t *syn*	48.5	−27	180	59	222	39	42.2	−21	−179	179	217	40	48.0	−34	−178	−73	214	40

[a] Total energy in kJ/mol; [b] χ (O4′-C1′ − N1-C2), γ (O5′-C5′-C4′-C3′), ϵ_1 (C2′-C1′-$\underline{C}H_2$-$\underline{O}H$), P and Ψ_m are expressed in degrees.

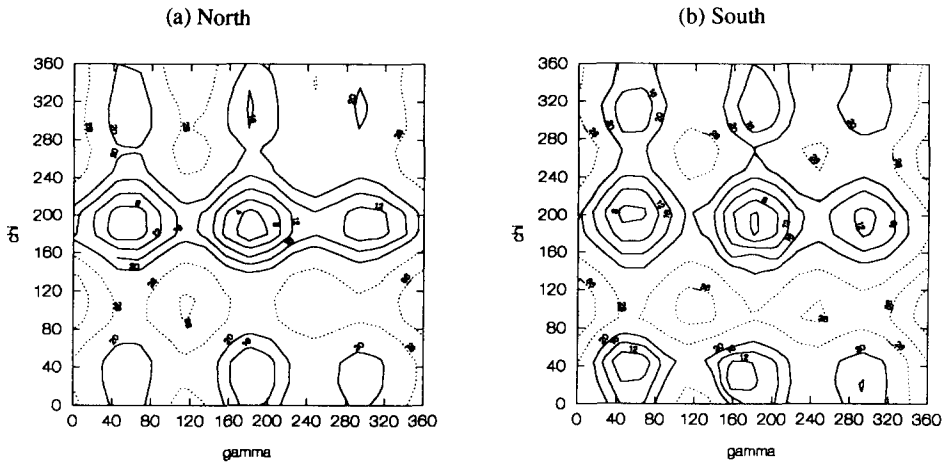

Fig. 5. Plot of energy contours in χ (O4′-C1′-N9-C2)-γ (O5′-C5′-C4′-C3′) plane for CNT (**6**). At every point of potential energy surface the whole molecule was fully optimized, except the orientation of 3′-OH and 2′-OH groups which were restrained to geometry where 3′-O $\cdots$ H-O2′ hydrogen bond is possible (ϵ_3 and ϵ_2 were constrained in addition to χ and γ which were varied during grid searches of the conformational space). The contours show the lowest energy minimum at $\chi = 180°$ and $\gamma = 60°$ for the North type puckered sugar moiety in **6** (panel a; $E = 31.0$ kJ/mol) and at $\chi = 180°$ and $\gamma = 180°$ only 0.6 kJ/mol above (panel a; $E = 31.6$ kJ/mol). The South conformers of CNT (**6**) have the lowest energy minima at $\chi = 200°$ and $\gamma = 60°$ (panel b; $E = 31.7$ kJ/mol) and at $\chi = 180°$ and $\gamma = 180°$ which has 1.0 kJ/mol higher energy (panel b; $E = 32.7$ kJ/mol). In both graphs the energy contours represented with solid line are spaced by 4.0 kJ/mol and are shown up to 20.0 kJ/mol above the lowest energy minimum in that region of conformational space. The energy contours shown by dotted line start at 28.0 kJ/mol above the lowest energy minimum in that region and are incremented by 8.0 kJ/mol.

thymine moiety. Molecular mechanics calculations gave the lowest energy structure with ϵ_1 (C2′-C1′-*C*H$_2$-*O*H) in *trans* orientation (Table 4). The energetic preference of ϵ_1^t over $\epsilon^+{}_1$ and $\epsilon^-{}_1$ in the (North-γ^+-*anti*) and (North-γ^t-*anti*) regions of conformational space (major conformers as observed by NMR) is approx. 9 and 14 kJ/mol, respectively (Table 4).

TABLE 5
Local minima established for 1-(1′-cyano-β-D-ribofuranosyl)thymine (CNT) (**6**)

Entry	Conformer	*anti*					Entry	*syn*				
		E [a]	χ [b]	γ	P	Ψ_m		E [a]	χ [b]	γ	P	gJ_m
1	N γ^+	29.9	−172	58	17	41	7	41.0	−57	60	−28	41
2	N γ^t	30.6	−172	−178	12	41	8	40.2	45	−178	54	41
3	N γ^-	35.3	−172	−64	9	41	9	44.8	45	−64	55	40
4	S γ^+	31.5	−163	58	150	37	10	37.0	−56	57	139	42
5	S γ^t	32.3	−166	−179	188	37	11	38.6	−56	−178	136	42
6	S γ^-	36.6	−165	−65	182	37	12	41.6	−56	−64	136	42

[a] Total energy in kJ/mol; [b] χ (O4′-C1′-N1-C2), γ (O5′-C5′-C4′-C3′), P and Ψ_m are expressed in degrees.

Experimentals

^{1}H-NMR spectra were recorded on 500 MHz Bruker AMX NMR spectrometer in D_2O. 1-D ^{1}H nOe difference spectroscopy was performed with preirradiation of 5s with an irradiation power of 40dB. Force field calculations were performed using MacroModel software package [12].

1-(1,3,4,6-tetra-O-benzoyl-β-D-psicofuranosyl)thymine

2,4-bis(trimethylsiloxy)thymine (400 mg, 1.5 mmol) was added to a solution of 1,2,3,4,6-penta-*O*-benzoyl-β-D-psicofuranose (0.73 mmol) in acetonitrile (4.5 ml) under a nitrogen atmosphere. After cooling the mixture in an ice bath, stannic chloride (0.2 ml) was added dropwise with vigorous stirring. The orange homogenous solution was stirred for 1h at 20°C. After removal of the solvent in vacuo the residue was dissolved in methylene chloride and the solution was shaken with saturated aqueous sodium bicarbonate. The resulting emulsion was filtered over a layer of celite. The organic phase was separated and evaporated under reduced pressure. The residue was then purified by silica gel column chromatography with 1:1 (v/v) ethyl acetate-hexane as eluent to afford the titled nucleoside (370 mg, 68%). $R_f = 0.32$ (AcOEt:hexane = 1:1), $[\alpha]_D^{20} = -34°$ ($c = 0.65$, $CHCl_3$), UV (95% EtOH): $\lambda_{max} = 267$ nm ($\epsilon = 7600$), ^{1}H-NMR ($CDCl_3$, 300 MHz) δ: 8.13–7.29 (m, 21 H, Ar and H6), 6.64 (d, 1 H, H3′, $J_{3'4'} = 5.5$ Hz), 6.00 (m, 1 H, H4′), 5.15 (d, 1 H, H1′a, $J_{gem} = 12$ Hz), 5.04 (dd, 1 H, H6′a, $J_{5'6'a} = 3.0$ Hz, $J_{gem} = 13$ Hz), 4.99 (d, 1 H, H1′b), 4.94 (m, 1 H, H5′), 4.40 (dd, 1 H, H6′b, $J_{5'6'b} = 3.0$ Hz), 1.67 (s, 3H, Me) ppm.

1-(β-D-psicofuranosyl)thymine (5 HMT)

A suspension of blocked nucleoside (0.5 mmol) in a mixture of methanol (3.7 ml) and concentrated aqueous ammonia (5.8 ml) was stirred at room temperature for 24h. The homogeneous solution was lyophilized and the crude product was purified by column chromatography (CH_2Cl_2: MeOH = 70:30). HMT (**5**) was obtained in 77% yield. $R_f = 0.34$ ($CHCl_3$: MeOH = 7:3), $[\alpha]_D^{20} = -22°$ ($c = 1.08$, MeOH), UV (95% EtOH): $\lambda_{max} = 268$ nm ($\epsilon = 6883$).

Acknowledgements

Authors thank Swedish Board for Technical Development, Swedish Natural Science Research Council and Medivir AB (Stockholm) for generous financial supports and Wallenbergstiftelsen, Forskningsrådsnämnden (FRN) and University of Uppsala for funds for the purchase of a 500 MHz Bruker AMX NMR spectrometer. Authors (V.B and A.G) thank CNRS (URA 463) for generous financial support and RHÔNE-POULENC RORER for a studentship.

Reference

1a Hoshino, H., Shimizu, N., Shimada, N., Takita, T. and Takeuchi, T. (1987) J. Antibiot. 40, 1077.
1b Seki, J., Shimada, N., Takahashi, K., Takita, T., Takeuchi, T. and Hoshino, H. (1989) Antimicrob. Agents Chemother. 33, 773.
1c Shimada, N., Hasegawa, S., Saito, S., Nishikiori, T., Fujii, A. and Takata, T. (1987) J. Antibiot. 40, 1788.
2 Tseng, C.K.-H., Marquez, V.E., Milne, G.W.A., Wysocki, R.J., Mitsuya, H., Shirasaki, T. and Driscoll, J.S. (1991) J. Med. Chem. 34, 343.
3 Suhadolnik, R.J. (1970) Nucleoside Antibiotics, Wiley, New York.
4 Suhadolnik, R.J. (1979) Nucleosides as Biological Probes, Wiley, New York.
5 Haasnoot, C.A.G., de Leeuw, F.A.A.M., de Leeuw, H.P.M. and Altona, C. (1979) Recl. Trav. Chim. Pays-Bas 98, 576.
6a Altona, C. and Sundaralingam, M. (1972) J. Am. Chem. Soc. 94, 8205.
6b Altona, C. and Sundaralingam, M. (1973) J. Am. Chem. Soc. 95, 2333.
7a de Leeuw, F.A.A.M. and Altona, C. (1983) J. Comp. Chem. 4, 438.
7b de Leeuw, F.A.A.M. and Altona, C. (1983) PSEUROT: QCPE Program No. 463.
8 de Leeuw, H.P.M., Haasnoot, C.A.G. and Altona, C. (1980) Isr. J. Chem. 20, 108.
9 Rinkel, L.J. and Altona, C. (1987) J. Biomol. Struct. Dyn. 4, 621.
10 Haasnoot, C.A.G., de Leeuw, F.A.A.M., de Leeuw, H.P.M. and Altona, C. (1981) Org. Magn. Reson. 15, 43.
11 Saenger, W. (1984) In: Principles of Nucleic Acid Structure, Springer Verlag, New York.
12 Still, W.C. et al. (1992) MacroModel V3.5a, Columbia University, New York.
13 Mohamadi, F., Richards, N.G.J., Guida, W.C., Liskamp, R., Lipton, M., Caufield, C., Chang, G., Hendrickson, T. and Still, W.C. (1990) J. Comp. Chem. 11, 440.
14 Lipton, M. and Still, W.C. (1988) J. Comp. Chem. 9, 343.
15 Ponder, J.W. and Richards, F.M. (1987) J. Comp. Chem. 8, 1016.
16 Davies, D.B. (1978) Progress in NMR Spectroscopy, Pergamon Press, 12, 135.
17 Plavec, J., Buet, V., Grouiller, A., Koole, L.H. and Chattopadhyaya, J. (1991) Tetrahedron 47, 5847.
18 Plavec, J., Koole, L.H. and Chattopadhyaya, J. (1992) J. Biochem. Biophys. Methods 25, 253.
19 Lesyng, B. and Saenger, W. (1984) Carboh. Res. 133, 187.
20 Singh, U.C. and Kollman, P.A. (1984) J. Comp. Chem. 5, 129.
21 Besler, B.H., Merz, K.H. and Kollman, P.A. (1990) J. Comp. Chem. 11, 431.
22 Weiner, S.J., Kollman, P.A., Nguyen, D.T. and Case, D.A. (1986) J. Comp. Chem. 7, 230.
23 Frish, M.J., Trucks, G.W., M. Head-Gordon, Gill, P.M.W., Wong, M.W., Foresman, J.B., Johnson, B.G., Schlegel, H.B., Robb, M.A., Replogle, E.S., Gomperts, R., Andres, J.L., Raghavachari, K., Binkley, J.S., Gonzales, C., Martin, R.L., Fox, D.J., Defrees, D.J., Baker, J., Stewart, J.J.P. and Pople, J.A. (1992) Gaussian 92, Revision A, Gaussian, Pittsburgh, PA.
24 Izatt, R.M., Hansen, L.D., Rytting, J.H. and Christensen, J.J. (1965) J. Am. Chem. Soc. 87, 2760.
25 Birnbaum, G.I., Giziewicz, J., Huber, C.P. and Shugar, D. (1976) J. Am. Chem. Soc. 98, 4640.